Title

Modeling potential air temperature reductions yielded by cool roofs and urban irrigation in the Kansas City Metropolitan Area

Authors

Jeong, Seongeun

Millstein, D

Levinson, R

Publication Date

2021-05-01

DOI

10.1016/j.uclim.2021.100833

Modeling potential air temperature reductions yielded by cool roofs and urban irrigation in the Kansas City Metropolitan Area

Seongeun Jeong, Lawrence Berkeley National Laboratory (USA)*
Dev Millstein, Lawrence Berkeley National Laboratory (USA)
Ronnen Levinson, Lawrence Berkeley National Laboratory (USA)

**Corresponding author: Seongeun Jeong (sjeong@LBL.gov)*

ABSTRACT

We evaluate two mitigation strategies for urban heat island (UHI) in the Kansas City Metropolitan Area (KCMA). Using the Weather Research and Forecasting (WRF) model, we assess the potential benefits of reflective cool roofs and urban irrigation on air temperature in typical summer conditions between 2011 and 2015, and during six of the strongest historical heat waves during 2005 – 2016. Under the typical summer conditions, we simulate 2-m air temperature for 10 summer weeks, finding average daytime (07:00 – 19:00 local time) temperature reductions of 0.08 and 0.28 °C for cool roofs and urban irrigation, respectively. During the six heat-wave episodes, we find similar daytime temperature reductions of 0.02 and 0.26 °C for the two scenarios compared to those of the typical summer conditions. Our results suggest that urban irrigation can be more efficient than cool roofs in mitigating UHI in metropolitan regions where the majority of the land cover is comprised of areas with low urban (i.e., non-vegetated) fractions. Finally, we find the alteration of surface conditions due to enhanced roof albedos influences precipitation within the WRF simulation, in particular during the heat waves. Further research would be necessary to determine the robustness of this last finding.

1. Introduction

Temperatures in urban regions are increasing due to a combination of global climate change and local factors such as the use of heat-trapping materials and anthropogenic heat sources (Hassid et al. 2000; Miller et al. 2008; Salamanca et al. 2013). A recent study in North America suggests that urban expansion alone can increase regional temperature at a level similar to warming due to the increase of greenhouse gases in the atmosphere (Georgescu et al. 2014). In addition, the temperature increase in urbanized areas is known to be a source of air quality problems (Nazaroff 2013) and heat-related public health problems (Luber and McGeehin 2008; Li and Bou-Zeid 2013).

Carefully planned urban growth strategies may provide an opportunity to mitigate urban heat stress. Increasing the solar reflectance (albedo) of roofs can cool buildings, reducing air conditioning use, and lowering urban air temperatures (Parker and Barkaszi 1997; Akbari et al. 1999; Levinson et al. 2005; 2010; Vahmani et al. 2016). A second strategy to mitigate urban heat stress is to irrigate the urban vegetated landscape. Urban irrigation can reduce the urban

temperature by increasing evaporative cooling of the surface and near-surface air (Vahmani and Hogue 2015; Vahmani and Ban-Weiss 2016).

In this work, we evaluate potential temperature reductions from both highly reflective "cool" roofs and urban irrigation in the Kansas City Metropolitan Area (KCMA), a major metropolitan area in the Midwestern region of the United States. We examine air temperature reductions from each of the two mitigation strategies. We also show the potential impact of changes in the land surface and near-surface atmospheric conditions on air temperature over the study domain. This study tests the impacts of full, idealized implementation of the mitigation strategies. In the case of urban irrigation, urban irrigation serves as a surrogate for a strategy that supports stormwater infiltration practices via green infrastructure.

2. Method

2.1. WRF Urban Canopy Model

We use the Weather Research and Forecasting (WRF) model (version 3.8, Skamarock et al. 2008) to simulate different urban heat island mitigation strategies. We use the single-layer urban canopy model (SLUCM, Kusaka et al. 2001; Kusaka and Kimura 2004) to represent the urban physics. We use the Noah land surface model (LSM) (Chen and Dudhia 2001), following a number of urban modeling studies (e.g., Millstein and Menon 2011; Salamanca et al. 2013; Cao et al. 2015; Vahmani and Ban-Weiss 2016 et al.) The main physical options for WRF-SLUCM simulations in this study are set as follows: (1) radiation: Rapid Radiative Transfer Model scheme (Mlawer et al. 1997) for longwave radiation and Dudhia scheme (Dudhia 1989) for the shortwave; (2) planetary boundary layer: UW scheme (Bretherton and Park, 2009); and (3) microphysics: Morrison double-moment scheme (Morrison et al. 2009). The initial and boundary conditions are provided by the North American Regional Reanalysis (Mesinger et al. 2006). A two-way nesting scheme for the three-level domains (13.5, 4.5, and 1.5 km) is used for the meteorology simulations (Figure 1). The atmosphere is divided into a total of 30 levels.

Figure 1 shows the entire modeling domain and the 1.5-km inner domain that includes KCMA. The National Land Cover Data (NLCD; Homer et al. 2015), which provides forty land cover types, is utilized to define land type in the study domains (Figure 1). The summary for KCMA's meteorology and geography is presented in the Supporting Information (SI; Text S1). We adopt the default urban fractions of 50%, 90%, and 95% for the three urban types: low, medium and high development intensity, respectively. To better represent the urban canopy in WRF simulations, we use the urban parameter data (e.g., mean building height) from the National Urban Database and Access Portal Tool (NUDAPT, Ching et al. 2009). Because the NUDAPT dataset was available only for the urban core area of KCMA, we extrapolate the existing dataset to cover the entire KCMA. In this extrapolation, we calculated median values by development intensity (i.e., low, medium, and high) from the available NUDAPT dataset and applied them to non-NUDAPT areas. Using a spin-up of 18 hours, we simulate meteorological variables including 2-m temperature in typical summer conditions between 2011 and 2015 and during six of the strongest historical heat wave events over the past 12 years (2005 – 2016). Results from the spin-up period are not included in the subsequent analysis. The diagnostic 2-m

temperature (hereinafter "air temperature") variable in WRF-SLUCM represents an air temperature near the height of the urban canopy (Li and Bou-Zeid 2014).

2.2. Mitigation Strategies for WRF Simulations

We run a series of simulations to evaluate urban temperature reductions in KCMA upon raising roof albedo, and upon increasing urban irrigation. We simulated 10 summer weeks representing typical summer conditions, selecting the 15th – 21st of July and August in 2011 – 2015. Separately, we identified and simulated six of the strongest historical heat-wave events over the past decade (2005 – 2016). For historic heat waves, we identified the episodic heat wave periods using measured near-surface air temperature data at the C. R. Wheeler Downtown Airport located in the urban area of KCMA, which are available from the Integrated Surface Database (ISD) of NOAA's National Centers for Environmental Information (NCEI, 2017). We selected six heat wave episodes by finding the periods with the highest seven-day moving average temperatures during 2005 – 2016 (see Table S1 in the SI). For 2012, we identified two heat waves but selected the stronger episode in early July. For each 7-day episode, we conduct independent WRF simulations for two mitigation scenarios: raising roof albedo and increasing urban irrigation. Within the cool roof scenario, roof albedo is raised from 0.20, its value in the control scenario, to 0.60, following Cao et al. (2015). For the irrigation scenario, we activate the WRF irrigation scheme, inactive in the control case, which causes the top two model layers to reach critical moisture content such that transpiration is not limited by water availability. The WRF irrigation scheme is implemented at 21:00 local standard time (LST) every day from May to September.

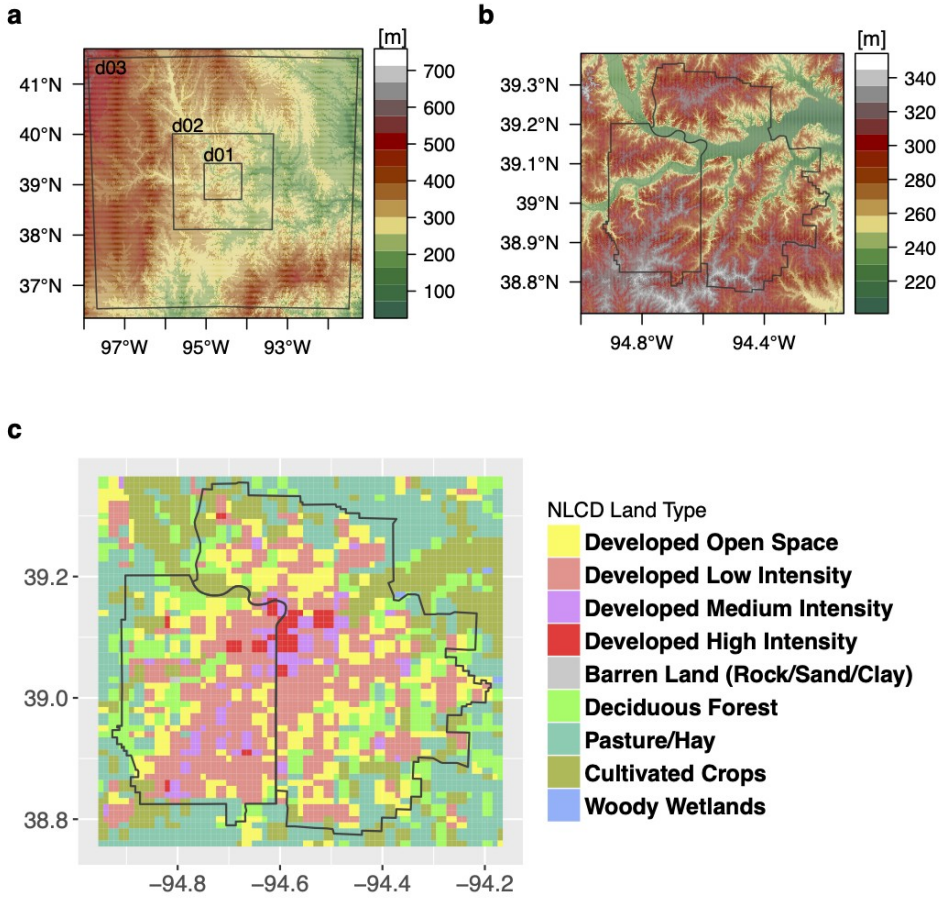

Figure 1. Maps showing (a) elevation of the entire modeling domain, at a horizontal resolution of 1 arc-second (~30 m) (National Map, 2017); (b) elevation of inner modeling domain (see Figure S1 in the SI for an enlarged elevation plot on a Google Map); and (c) land type (Homer et al. 2015). Boxes d01, d02, and d03 in panel *a* represent WRF modeling outer (d01) and nested (d02 and d03) domains, while the boundary (black solid line) in panels *b* and *c* represents the urbanized area in the Kansas City metropolitan region from the 2000 U.S. Census (Mid-America Regional Council, 2017).

3. Results and Discussion

3.1. Evaluation of Heat Island Mitigation Strategies

We use 2-m temperature simulations from WRF-SLUCM to evaluate the impact of heat island mitigation strategies. To check the performance of WRF using the set-up described in Section 2.1, we compare WRF-simulated near-surface (2-m) temperature with observations from two ISD surface stations: Charles B. Wheeler Downtown Airport (CBWDA) and Johnson County Executive Airport (JCEA) (for locations, see Figure S2 in the SI). Overall, WRF simulations for CBWDA are well-correlated with observed temperature yielding values of 0.82 and 0.76 for the coefficient of determination (i.e., r^2) during normal and heat wave episodes, respectively (see Figure S3 in the SI). Compared to observations, WRF simulations at CBWDA

show 2.2 °C and 2.1 °C biases (WRF minus observation) for normal and heat wave periods, respectively (Figure S3). The r^2 values for JCEA were similar, yielding 0.83 for both normal and heat wave periods. WRF overestimates 2-m temperature by 3.1 °C and 2.7 °C at JCEA. The mean absolute error (MAE) ranges from 2.4 to 3.2 °C, depending on the observation site and episode (Figure S3). We found that average (i.e., arithmetic mean) temperatures across KCMA during both normal and heat wave conditions were sensitive to elevation, with lower elevations having higher temperatures; for example, compare the temperature maps in Figure 2a,b to the elevation map in Figure 1b. However, the spatial patterns of temperature reductions from the two mitigation scenarios, for both normal and heat wave episodes, match the land-use type distribution; that is, the larger temperature reductions (Figure 2c-f) correlate with the higher density development land-use types (Figure 1c). We note that most of the high-intensity development is located near the river and at low elevation relative to the surrounding areas. Thus the influence on temperature mitigation strategies of land-use type cannot be fully separated from the influence of topography.

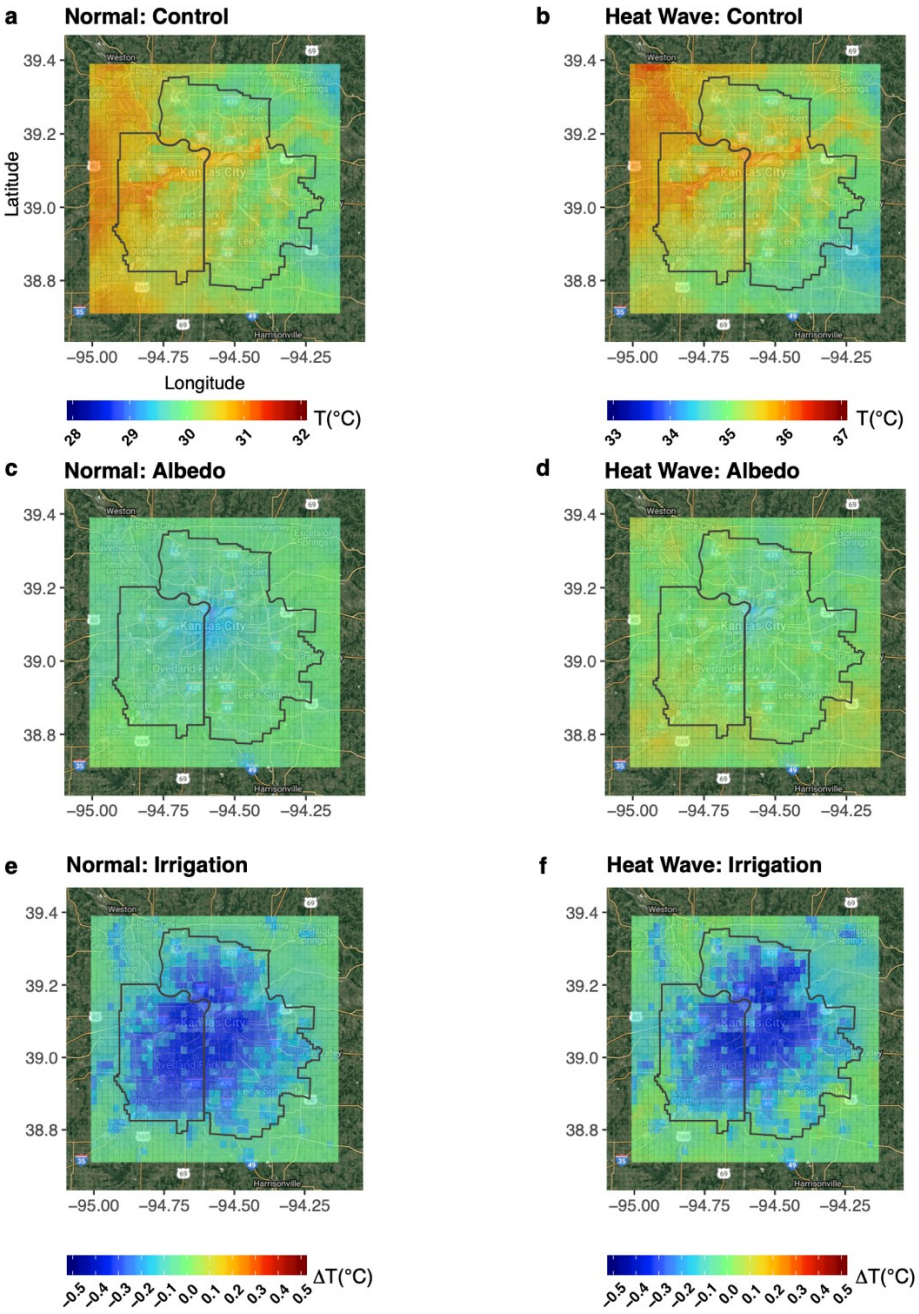

Figure 2. (a, b) Simulated average daytime (07:00 – 19:00 LST) 2-meter air temperature. (c-f) Temperature difference (°C, mitigation minus control) due to roof albedo and urban irrigation mitigation scenarios for the normal and heat wave episodes.

The average daytime (07:00 – 19:00 LST) temperature reductions from the mitigation scenarios vary by urban development intensity (Figure 3). For the roof albedo scenario, the average temperature reduction for the normal episode ranges from 0.07 to 0.17 °C depending on the development intensity. For the heat wave episode, the temperature reductions vary from 0.01 to 0.09 °C, showing somewhat reduced mitigation effect compared to that of the normal episode

(Figure 3a). Recall that in Figure 3, the summary statistics for the temperature reduction are presented by urban development density. This result is different from that reported in Cao et al. (2015) where they reported significantly larger temperature reductions from cool roofs during heat waves compared to normal summer conditions. The absence of increased temperature reductions during heat waves in the current work counters the generalization of a simple hypothesis that could be derived from Cao et al. (2015)—namely, that urban mitigation strategies will produce larger temperature reductions given higher initial temperatures. This indicates that the city's geography and regional meteorology conditions can influence the performance of mitigation strategies (e.g., diminish the temperature reduction attained) during extreme conditions such as heat waves. Variations in urban geometry (roof width, canyon width, and building height) could further contribute to differences in outcomes (Zhang et al. 2018). We expand this discussion in later sections.

Temperature reductions from the urban irrigation scenario (Figure 3b) are consistently larger than those of the roof albedo scenario for all development intensity types with mean temperature reductions being equal to or larger than 0.2 °C for all cases. As shown in Figure 3b, the interquartile ranges (IQR, or difference between upper and lower quartiles) for the normal and heat wave episodes overlap, suggesting that there is likely no significant difference in the effect of temperature reductions between the normal and heat wave episodes.

We applied the nonparametric Wilcoxon-Mann-Whitney test (WMW) (Mann and Whitney 1947) to decide whether there is a statistically significant difference in the mean temperature between the control and mitigation scenarios. Using the WMW test, we can evaluate whether the population distributions are identical without normality assumptions for the data. For this test, we assumed that each of the control and mitigation scenarios is an independent group for which we can estimate the mean air temperature. As indicated by the IQR in the boxplots of Figure 3, the WMW test determined that, except for the roof albedo scenario during the heat wave episode, the temperature in each mitigation scenario was significantly different from that in the control case (p-value much less than 0.05). A significant result indicates that those mitigation cases were effective in lowering air temperature in KCMA.

Figure 3a shows that the mean daytime temperature reductions from the cool roof scenario across KCMA (i.e., the three development intensity areas combined) are 0.08 and 0.02 °C for the normal and heat wave episodes, respectively. The magnitude of temperature reductions from our cool roof simulation is smaller than those reported by Cao et al. (2015) and Vahmani et al. (2016). However, we note that air temperature depends on many factors including the land surface conditions (e.g., level of urbanization) and influence from outside the urban area (e.g., sea breeze), as well as the assumption about the cool roof albedo. For example, Vahmani et al. (2016) reported a daytime temperature reduction of 0.9 °C from the adoption of cool roofs in Southern California where the combined industrial and commercial area accounts for 33% % of the total cooling. We note that although the land classification method of our study does not exactly match that of Vahmani et al. (2016), our high development area accounts for only 5% of KCMA, which is much smaller than the industrial/commercial area fraction used in their work. Cao et al. (2015) showed that the temperature reduction from a similar cool roof scenario was larger during the heat wave episodes than during the normal episodes, while our result shows a higher temperature reduction during the normal periods than the heat wave. Possible reasons for this are discussed in Section 3.3.

The cooling effects of daily irrigation at 21:00 LST on daytime temperatures (07:00 – 19:00 LST) are evident over all three urban types for both the normal and heat wave episodes (Figure 3b). The decrease in the air temperature from urban irrigation is largely due to increased evaporation. The mean temperature reduction for the normal episodes ranges from 0.21 to 0.29 °C while the heat wave episodes also show a similar range of temperature reduction (0.20 - 0.29 °C). The urban irrigation reduced average daytime temperatures across KCMA by 0.28 and 0.26 °C for the normal and heat wave episodes, respectively (Figure 3b). The high development area had the lowest effect of the irrigation strategy on the temperature reduction. Considering that many parts of KCMA are irrigated already, we note that our estimate for the temperature reduction due to urban irrigation (at the critical moisture content level) is likely an upper bound.

To provide a more complete picture of the statistical distribution of the simulated temperature differences from the adoption of different mitigation strategies, we show histograms of pixel-level temperature changes. Figure 4 shows histograms for daytime temperature changes (ΔT, mitigation minus control) from all mitigation scenarios by development intensity for both the normal and heat wave episodes. For the roof albedo scenario, the high development intensity area shows the largest temperature reduction (i.e., ΔT) for both the normal and heat wave episodes. This result is expected because the high development area, on average, is associated with a larger roof area ratio within a given grid pixel. Also, the range of ΔT in the high development area is larger than those of the medium and low development areas, showing larger variability in temperature reductions.

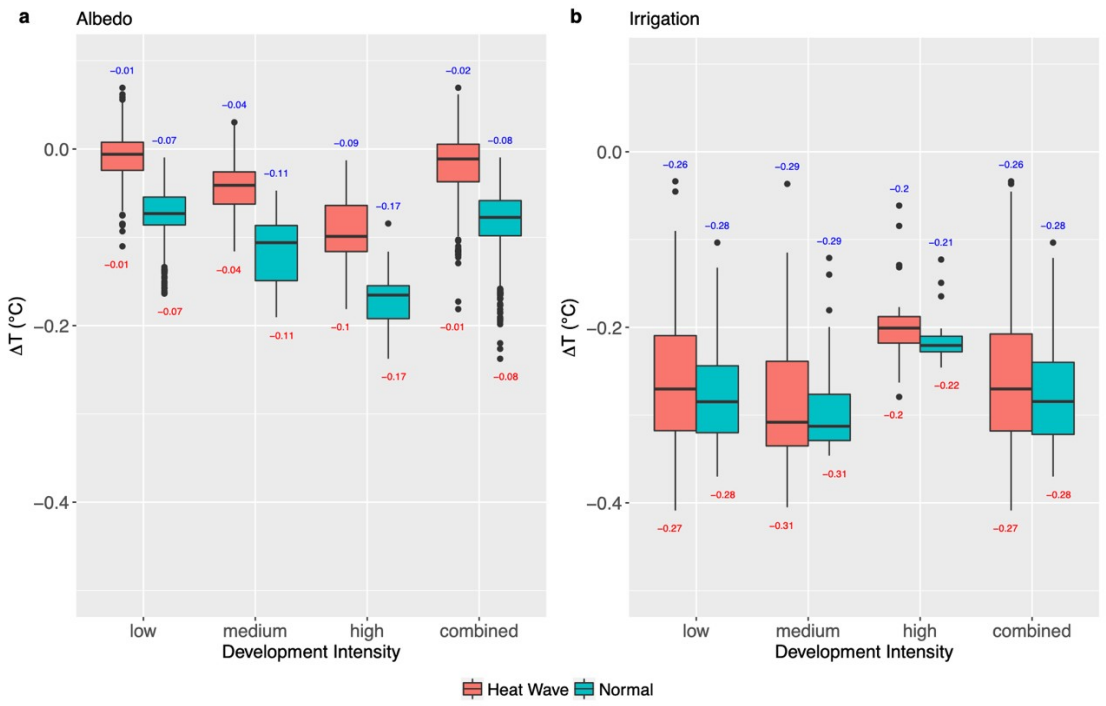

Figure 3. Boxplots of simulated daytime (07:00 – 19:00 LST) air temperature differences (ΔT, mitigation minus control) for (a) roof albedo, and (b) urban irrigation. For each scenario, the boxplot is shown for the low, medium and high development areas and the entire KCMA (i.e., "combined"). Note the combined area has results most similar to the most prevalent land area type (low), but shows the spread of results across all land area types. The numbers at the top of the box (blue text) and bottom of the box (red text) represent mean and median values of the data, respectively.

In KCMA, the low-development area has lots of open space and low roof area fractions (<10%). For both the normal and heat wave episodes, the high development density area shows the smallest temperature reduction from urban irrigation (Figure 4). This is likely because low and medium development intensity areas have larger available irrigated (urban vegetation) area fractions than do high development intensity areas. This result suggests that, at the regional level, the mitigation benefits from urban irrigation may be maximized when focusing more on the low and medium development intensity areas. We expect that irrigation strategies can be implemented more easily in the low and medium development intensity areas than in the high development area. For some cases (e.g., the albedo scenario for medium development areas during the normal episodes shown in Figure 4a), the distribution of ΔT is bimodal, suggesting that there is spatial variability in the effect of mitigation strategies within the same development intensity. Characterizing this spatial variability with a similar development level through future studies could improve mitigation planning. Using additional land cover categories for detailed characterization of land surfaces could be useful in understanding the urban heat island and evaluating the mitigation strategies applied.

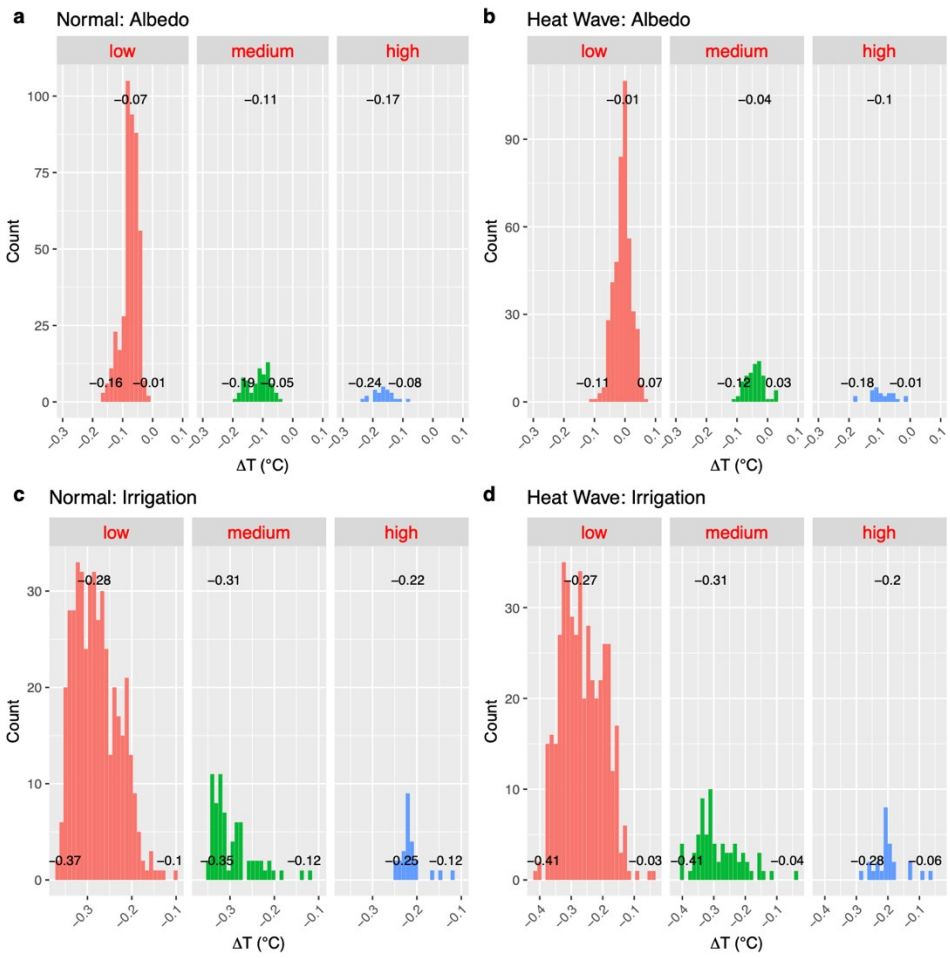

Figure 4. Histogram of pixel-level daytime (07:00 – 19:00 LST) temperature differences (°C) by mitigation scenario for the normal (a and c) and heat wave (b and d) episodes. "Albedo" and "irrigation" in the plot titles denote the cool roof albedo and urban irrigation mitigation scenarios, respectively. The numbers at the bottom of each plot represent the minimum and maximum ΔT values within the boundary of KCMA. The number at the top of each plot shows the median ΔT value.

3.2. Diurnal Cycles of Mitigation Effects

Cool roofs and urban irrigation produce different diurnal patterns of cooling in KCMA (Figure 5). During normal episodes, cool roofs provide peak cooling during the middle of the night, whereas urban irrigation provides the most cooling during the daylight hours. During heat waves, we see the largest cooling impacts during the late evening hours. During heat waves we see increased temperatures under both the cool roof and urban irrigation scenarios during the late afternoon and early evening hours. Both the later afternoon temperature increases and the early morning temperature reductions are potentially related to changes in local meteorological patterns, including a decrease in precipitation that was found in the cool roof mitigation scenario during the heat wave episodes (see Section 3.3.).

Urban irrigation (irrigated at 21:00 LST) reduces temperatures more during the daytime and evening than in the early morning (Figure 5). In particular, we note the small temperature

reduction from urban irrigation during the early morning hours prior to sunrise for the normal episode. This is likely due to higher upward ground heat fluxes during the night. Vahmani and Ban-Weiss (2016) suggest that irrigation-induced increased soil moisture and subsequent soil heat conductivity lead to higher upward ground heat fluxes during the night. They show that when irrigated, both surface and air temperatures increase during the night compared to the non-irrigated case.

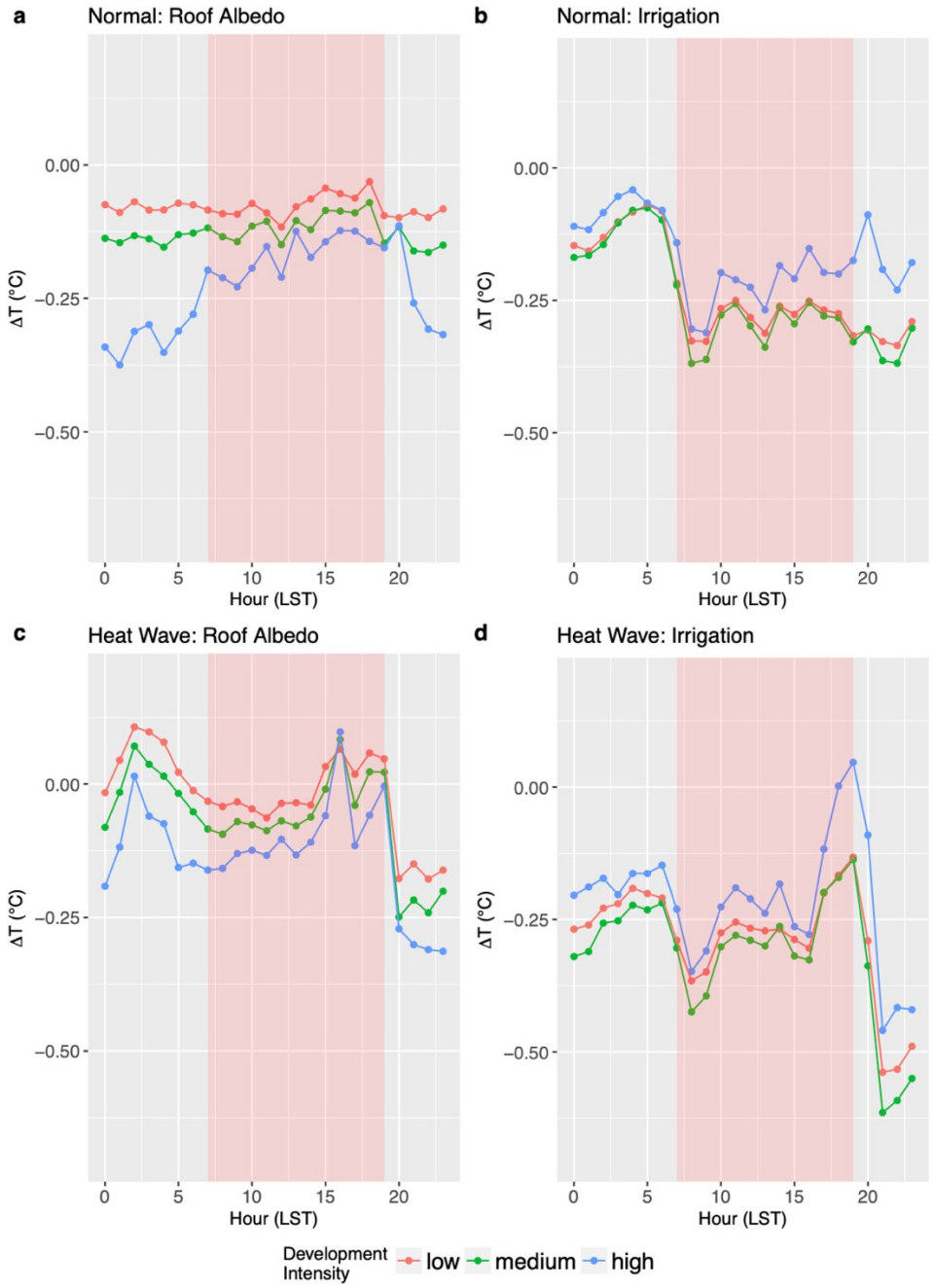

Figure 5. Diurnal cycles of differences in the air temperature (ΔT, mitigation minus control) for the mitigation strategies during (a, b) normal episodes and (c, d) heat wave episodes. The shaded region in light red shows the hours of sunlight (07:00 – 19:00 LST).

3.3. Impact of Mitigation Strategies on Local Weather

Figure 6a shows the simulated average air temperature for the control case and the cool roof albedo scenario during mid-afternoon through early evening hours (15:00 – 19:00 LST) in the heat wave episodes. Note that temperature values in Figure 6a are the average during the

hours when ΔT (mitigation minus control) is positive. In Figure 6a, the average air temperature is higher in the cool roof albedo scenario than in the control case, which was also shown in the diurnal cycle of ΔT for the cool roof scenario during the heat wave episodes (see Figure 5c). We explored a few meteorological variables related to air temperature (see Figure S5 in the SI for the diagnostic variables) and found that simulated precipitation is reduced in the cool roof scenario from 15:00 to 19:00 LST during the heat wave episodes (Figure 6b), likely causing the corresponding increase to air temperature. We note that temperature increase and precipitation decrease in the cool roof scenario relative to the control case are consistent across the study area. However, the spatial distribution of the difference in latent heat does not exactly follow that of the difference in precipitation.

We also compared observed surface meteorological conditions (temperature, wind speed, and precipitation) based on the two surface stations (see Figure S2 for locations) between the normal and heat wave episodes. Among the three meteorological variables, we find that the mean precipitation during the heat wave episodes is significantly lower than that of the normal episodes (Figure S4). The mean precipitation values at CBWD and JCEA during the heat wave episodes were only 10% and 63% of those of the normal episodes, respectively (Figure S4). Although this comparison between the normal and heat wave periods shows a large difference in the precipitation, our analysis of observed precipitation does not explain the reduced precipitation from the albedo scenario (relative to the base scenario) during the heat wave episodes. In addition, we compared change in temperature (mitigation minus control) and change in precipitation (mitigation minus control) at the pixel level during the heat wave hours when the average change in temperature (across the grid pixels) is positive (Figure S6). Figure S6 shows that the change in precipitation is negative for most grid pixels, suggesting the albedo mitigation is associated with less precipitation than the base scenario. The fitted line from a linear model shows a general inverse relationship between change in temperature and change in precipitation, although it does not necessarily show cause and effect.

This change in precipitation may be an artifact of the WRF modeling, as the preliminary analysis indicates that the control scenario has a higher frequency of mid-afternoon through early evening precipitation compared to that of the North American Land Data Assimilation System (NLDAS), which incorporates the best available observations and reanalyses (Xia et al. (2012); see Figure S7 and S8 in the SI). Further study could improve our understanding of how urban form interacts with local meteorological patterns.

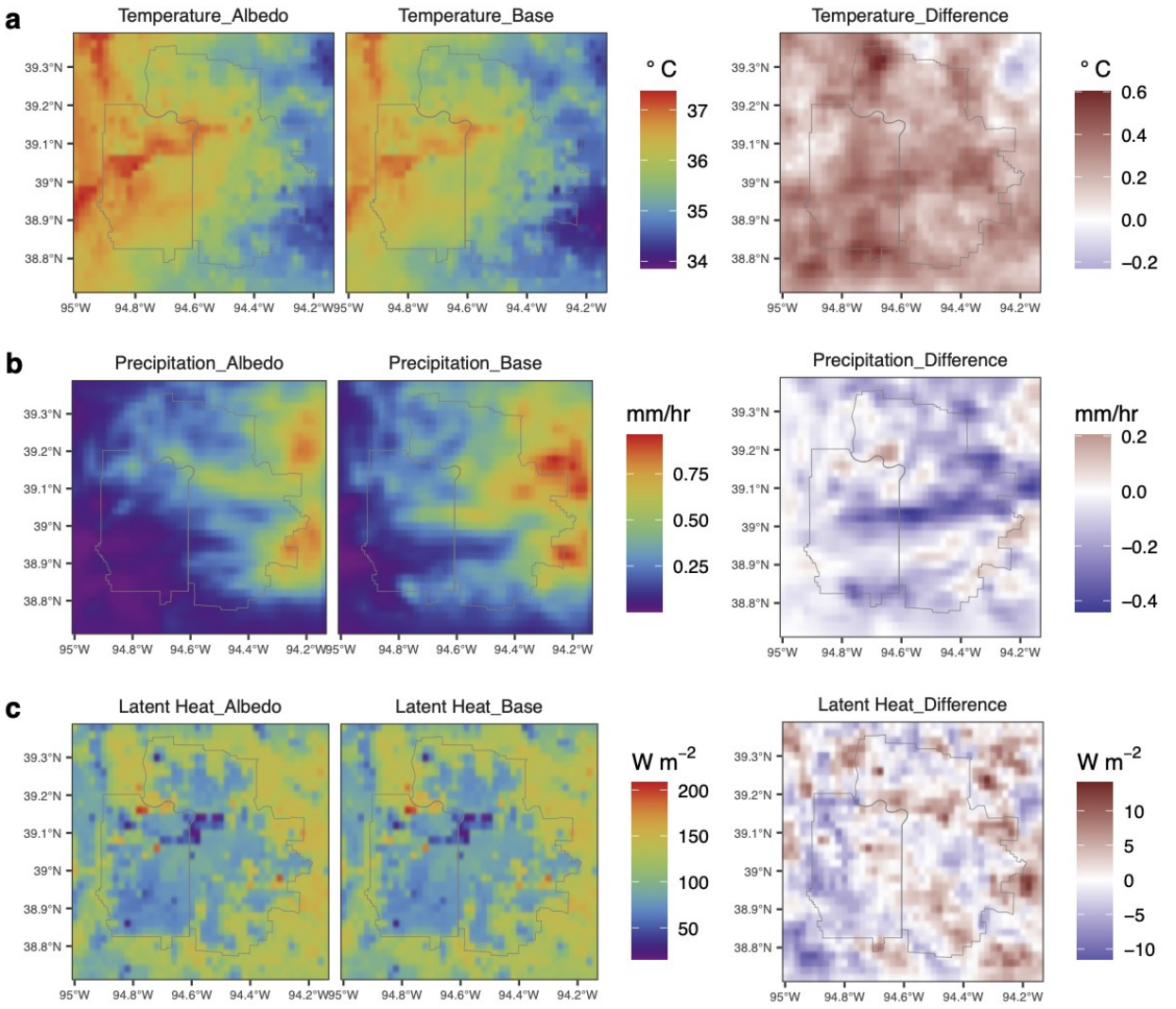

Figure 6. Comparison of mid-afternoon through early evening (15:00 – 19:00 LST) mean air temperature (a), non-convective precipitation (b), and latent heat (c) between the control case and the roof albedo scenario during the heat wave episodes. "base" and "albedo" denote the control and cool roof albedo cases, respectively. Note that the left two columns of panels *a*, *b*, and *c* show the average pixel values for each diagnostic variable (e.g., air temperature) during the hours when ΔT (mitigation minus control) is positive. The difference plot (right column) shows "albedo" minus "base."

4. Conclusions

We evaluated two UHI mitigation strategies in KCMA in typical summer conditions between 2011 and 2015, and during six of the strongest historical heat waves during 2005 – 2016. Using high-resolution meteorological model (WRF-SLUCM) simulations, we have shown that a policy of raising roof albedo by 0.40 in KCMA could reduce regional average daytime (07:00 – 19:00 LST) temperatures (evaluated at 2 m) by 0.08 and 0.02 °C for the normal summer

conditions and heat wave episodes, respectively. We found that daily urban irrigation at 21:00 LST could reduce average daytime temperature across the region by 0.28 °C and 0.26 °C for the normal and heat wave episodes, respectively. We also found that for the heat wave episode, temperature reductions from the albedo scenario might be larger during the early morning hours, but that a few hours of increased temperature could occur during the late afternoon and early evening as a result of decreased precipitation. We only observed the correlation between increased temperature and decreased precipitation (see Figure S6) during those afternoon to early evening hours for the albedo scenario. However, we could not establish causality between temperature and precipitation (or other meteorological variables), which is beyond the scope of our study. These particular patterns found during heat waves deserve additional study due to uncertainty about the interaction between cool roofs and precipitation.

Our results suggest that regions with relatively low roof area fractions such as KCMA may only see marginal air temperature benefits from reflective roofs although the benefit for the high development area is higher than the regional average. Most of the KCMA region (82%) is low development area, which has low roof area fractions (<10%), limiting the impact of reflective cool roofs on temperature reduction. Future studies of regions with low roof area fractions may be useful to verify our results. Compared to the reflective roof scenario, however, the urban irrigation scenario showed significantly larger temperature reductions, with average daytime temperature decreases of 0.28 and 0.26 °C for the normal and heat wave episodes, respectively. Though urban irrigation lowers temperature, it increases humidity, removing some of the thermal comfort benefits. These results suggest that for regions with low roof area fractions, urban irrigation may be a more effective heat island mitigation policy than raising roof albedo, although reflective roofs can still be helpful in highly developed areas. These results presume all roofs are available for albedo modification and that there is ample water availability for urban irrigation.

Acknowledgments

This research was supported by the Assistant Secretary for Energy Efficiency and Renewable Energy, State and Local Solution Center of the U.S. Department of Energy. It was also supported by Assistant Secretary for Energy Efficiency and Renewable Energy, Building Technologies Office of the U.S. Department of Energy under Contract No. DE-AC02-05CH11231. We would like to thank Linda Silverman, lead coordinator of the Climate Action Champions Initiative, for her management.

References

Akbari, H., Konopacki, S., & Pomerantz, M., 1999. Cooling energy savings potential of reflective roofs for residential and commercial buildings in the United States. *Energy*, 24(5), 391–407. https://doi.org/10.1016/S0360-5442(98)00105-4

Bretherton, C. S., Park, S., 2009. A new moist turbulence parameterization in the community atmosphere model. *Journal of Climate*, 22(12), 3422–3448. https://doi.org/10.1175/2008JCLI2556.1

Cao, M., Rosado, P., Lin, Z., Levinson, R., Millstein, D., 2015. Cool roofs in guangzhou, china: outdoor air temperature reductions during heat waves and typical summer conditions. *Environmental Science & Technology*, 49(24), 14672–14679. https://doi.org/10.1021/acs.est.5b04886

Chen, F., Dudhia, J., 2001. Coupling an advanced land surface–hydrology model with the Penn State–NCAR MM5 modeling system. Part I: Model implementation and sensitivity. *Monthly Weather Review*, 129(4), 569–585. https://doi.org/10.1175/1520-0493(2001)129<0569:CAALSH>2.0.CO;2

Ching, J., Brown, M., Burian, S., Chen, F., Cionco, R., Hanna, A., et al., 2009. National urban database and access portal tool. *Bulletin of the American Meteorological Society*, 90(8), 1157–1168. https://doi.org/10.1175/2009BAMS2675.1

Dudhia, J., 1989. Numerical study of convection observed during the winter monsoon experiment using a mesoscale two-dimensional model. *Journal of the Atmospheric Sciences*, 46(20), 3077–3107. https://doi.org/10.1175/1520-0469(1989)046<3077:NSOCOD>2.0.CO;2

Georgescu, M., Morefield, P. E., Bierwagen, B. G., Weaver, C.P., 2014. Urban adaptation can roll back warming of emerging megapolitan regions. *Proceedings of the National Academy of Sciences*, 111(8), 2909–2914. https://doi.org/10.1073/pnas.1322280111

Hassid, S., Santamouris, M., Papanikolaou, N., Linardi, A., Klitsikas, N., Georgakis, C., Assimakopoulos, D. N., 2000. The effect of the Athens heat island on air conditioning load. *Energy and Buildings*, 32(2), 131–141. https://doi.org/10.1016/S0378-7788(99)00045-6

Homer, C.G., Dewitz, J., Yang, L., Jin, S., Danielson, P., Xian, Coulston, J., Herold, N., Wickham, J., Megown, K., 2015. Completion of the 2011 National Land Cover Database for the conterminous United States – representing a decade of land cover change information. *Photogrammetric Engineering and Remote Sensing*, 81(5), 345-353. https://www.ingentaconnect.com/content/asprs/pers/2015/00000081/00000005/art00002

Kusaka, H., Kimura, F., 2004. Coupling a single-layer urban canopy model with a simple atmospheric model: impact on urban heat island simulation for an idealized case. *Journal of the Meteorological Society of Japan*, 82(1), 67–80. https://doi.org/10.2151/jmsj.82.67

Kusaka, H., Kondo, H., Kikegawa, Y., Kimura, F., 2001. A simple single-layer urban canopy model for atmospheric models: comparison with multi-layer and slab models. *Boundary-Layer Meteorology*, 101(3), 329–358. https://doi.org/10.1023/A:1019207923078

Levinson, R., Akbari, H., 2010. Potential benefits of cool roofs on commercial buildings: conserving energy, saving money, and reducing emission of greenhouse gases and air pollutants. *Energy Efficiency*, 3(1), 53–109. https://doi.org/10.1007/s12053-008-9038-2

Levinson, R., Akbari, H., Konopacki, S., Bretz, S., 2005. Inclusion of cool roofs in nonresidential Title 24 prescriptive requirements. *Energy Policy*, 33(2), 151–170. https://doi.org/10.1016/S0301-4215(03)00206-4

Li, D., Bou-Zeid, E., 2013. Synergistic interactions between urban heat islands and heat waves: the impact in cities is larger than the sum of its parts. *Journal of Applied Meteorology and Climatology*, 52(9), 2051–2064. https://doi.org/10.1175/JAMC-D-13-02.1

Li, D., Bou-Zeid, E., 2014. Quality and sensitivity of high-resolution numerical simulation of urban heat islands. *Environmental Research Letters*, 9(5), 055001. https://doi.org/10.1088/1748-9326/9/5/055001

Li, D., Bou-Zeid, E., Oppenheimer, M., 2014. The effectiveness of cool and green roofs as urban heat island mitigation strategies. *Environmental Research Letters*, 9(5), 055002. https://doi.org/10.1088/1748-9326/9/5/055002

Luber, G., McGeehin, M., 2008. Climate change and extreme heat events. *American Journal of Preventive Medicine*, 35(5), 429–435. https://doi.org/10.1016/j.amepre.2008.08.021

Mann, H. B., Whitney, D. R., 1947. On a test of whether one of two random variables is stochastically larger than the other. *The Annals of Mathematical Statistics*, 18(1), 50–60. https://doi.org/10.1214/aoms/1177730491

Mesinger, F., DiMego, G., Kalnay, E., Mitchell, K., Shafran, P. C., Ebisuzaki, W., et al., 2006. North american regional reanalysis. *Bulletin of the American Meteorological Society*, 87(3), 343–360. https://doi.org/10.1175/BAMS-87-3-343

Mid-America Regional Council, 2017. GIS Datasets, http://www.marc.org/Data-Economy/Maps-and-GIS/GIS-Data/GIS-Datasets (accessed in January 2017)

Miller, N.L., Hayhoe, K., Jin, J., Auffhammer, M., 2008. Climate, extreme heat, and electricity demand in California. *Journal of Applied Meteorology and Climatology*, 47(6), 1834–1844. https://doi.org/10.1175/2007JAMC1480.1

Millstein, D., Menon, S., 2011. Regional climate consequences of large-scale cool roof and photovoltaic array deployment. *Environmental Research Letters*, 6(3), 034001. https://doi.org/10.1088/1748-9326/6/3/034001

Mlawer, E.J., Taubman, S. J., Brown, P.D., Iacono, M.J., Clough, S.A., 1997. Radiative transfer for inhomogeneous atmospheres: RRTM, a validated correlated-k model for the longwave. *Journal of Geophysical Research: Atmospheres*, 102(D14), 16663–16682. https://doi.org/10.1029/97JD00237

Morrison, H., Thompson, G., Tatarskii, V., 2009. Impact of cloud microphysics on the development of trailing stratiform precipitation in a simulated squall line: comparison of one-

and two-moment schemes. *Monthly Weather Review*, 137(3), 991–1007. https://doi.org/10.1175/2008MWR2556.1

National Centers for Environmental Information, 2017. The Integrated Surface Database, https://www.ncdc.noaa.gov/isd (accessed in January 2017).

National Map, 2017. National Elevation Data, https://nationalmap.gov/elevation.html (accessed in January 2017).

Nazaroff, W.W., 2013. Exploring the consequences of climate change for indoor air quality. *Environmental Research Letters*, 8(1), 015022. https://doi.org/10.1088/1748-9326/8/1/015022

Parker, D. S., Barkaszi, S.F., 1997. Roof solar reflectance and cooling energy use: field research results from Florida. *Energy and Buildings*, 25(2), 105–115. https://doi.org/10.1016/S0378-7788(96)01000-6

Salamanca, F., Georgescu, M., Mahalov, A., Moustaoui, M., Wang, M., Svoma, B. M., 2013. Assessing summertime urban air conditioning consumption in a semiarid environment. *Environmental Research Letters*, 8(3), 034022. https://doi.org/10.1088/1748-9326/8/3/034022

Skamarock, W., Klemp, J., Dudhia, J., Gill, D., Barker, D., Wang, W., et al., 2008. A description of the Advanced Research WRF version 3. https://doi.org/10.5065/D68S4MVH

Vahmani, P., Ban-Weiss, G., 2016. Climatic consequences of adopting drought-tolerant vegetation over Los Angeles as a response to California drought: Climate Impacts Drought-Tolerant Plants. *Geophysical Research Letters*, 43(15), 8240–8249. https://doi.org/10.1002/2016GL069658

Vahmani, P., Hogue, T.S., 2015. Urban irrigation effects on WRF-UCM summertime forecast skill over the Los Angeles metropolitan area: urban irrigation and WRF-UCM modeling. *Journal of Geophysical Research: Atmospheres*, 120(19), 9869–9881. https://doi.org/10.1002/2015JD023239

Vahmani, P., Sun, F., Hall, A., Ban-Weiss, G., 2016. Investigating the climate impacts of urbanization and the potential for cool roofs to counter future climate change in Southern California. *Environmental Research Letters*, 11(12), 124027. https://doi.org/10.1088/1748-9326/11/12/124027

Xia, Y., Mitchell, K., Ek, M., Sheffield, J., Cosgrove, B., Wood, E., Luo, L., Alonge, C., Wei, H., Meng, J., Livneh, B., Lettenmaier, D., Koren, V., Duan, Q., Mo, K., Fan, Y., & Mocko, D. , 2012. Continental-scale water and energy flux analysis and validation for the North American Land Data Assimilation System project phase 2 (NLDAS-2): 1. Intercomparison and application of model products. *J. Geophys. Res.*, 117, D03109, https://doi.org/10.1029/2011JD016048

Zhang, J., Mohegh, A., Li, Y., Levinson, R., & Ban-Weiss, G., 2018. Systematic comparison of the influence of cool wall versus cool roof adoption on urban climate in the los angeles basin.

Environmental Science & Technology, 52(19), 11188–11197.
https://doi.org/10.1021/acs.est.8b00732